ADVANCED MATERIALS
www.advmat.de

www.MaterialsViews.com

Direct Transfer of Subwavelength Plasmonic Nanostructures on Bioactive Silk Films

*Dianmin Lin, Hu Tao, Jacob Trevino, Jessica P. Mondia, David L. Kaplan, Fiorenzo G. Omenetto, and Luca Dal Negro**

Silk fibroin[1] has emerged as a promising biopolymer interface for photonics and biomedical device applications due to its optical transparency,[2] mechanical robustness, biocompatibility,[3] biodegradability,[4] and ease of functionalization.[5] Moreover, silk fibroin has proven to be a biologically favorable carrier, enabling a new class of bioactive optical sensors, and providing added functionality and selectivity to conventional optical devices.[6] To date, various optical elements have been demonstrated using silk fibroin films, including waveguides,[7] microlens arrays and diffractive grating,[8] photonic crystals,[9] and optofluidic devices.[10]

However, the integration of the biocompatible silk materials platform with the emerging technology of subwavelength plasmonic nanostructures has not yet been demonstrated. In this paper, we demonstrate scalable and cost-effective replication of subwavelength plasmonic nanostructures directly onto functional silk biopolymers by a reusable transfer fabrication technique. In particular, we show high-fidelity sequential transfer of plasmonic nanoparticles, optical bow tie nanoantennas, and nanohole arrays with periodic and nonperiodic geometries, while preserving the functionality of the imprinted silk biopolymer. Broadband fluorescence enhancement and characteristic structural resonances in the visible spectral range are finally demonstrated using Rhodamine B (RhB) doped silk films directly imprinted with Vogel spiral arrays of Au nanoparticles.

Nanoplasmonics is the engineering of collective electron oscillations coupled to electromagnetic waves at metal-dielectric interfaces, metal nanoparticles, or nanoparticles aggregates.[11] These resonant oscillations, called surface plasmons, are strongly localized on the nanoscale and serve to boost optical cross sections in nanomaterials and the local intensity of electromagnetic fields, which are key attributes for the engineering of efficient optical devices.

Currently, the vast majority of nanoplasmonic structures are fabricated on semiconductors, quartz wafers, or polydimethylsiloxane (PDMS) substrates, which are poor biointerfaces lacking bioselectivity and functional programmability. Reliable and cost-effective integration of plasmonic nanostructures with functional silk films promises to open new avenues in bioactive nanophotonic devices for sensing and biomedical applications. However, the integration of complex plasmonic nanostructures with biopolymer films also poses unique challenges. Biopolymer films are solvent-sensitive organic materials, adding constraints to conventional nanofabrication techniques that often involve harsh processing conditions, high temperatures and pressures, energy radiation, wet chemicals or aggressive plasma etching processes. In addition, the successful development of plasmonic devices integrated with biopolymer materials requires scalable, cost-effective, and high throughput nanofabrication techniques capable of nanoscale spatial resolution.

Current nanoscale writing techniques, such as electron beam lithography (EBL), focused ion beam lithography (FIB), and scanning probe microscopy (SPM), suffer from high operating costs and low throughput. Shadow-mask patterning techniques, such as stencil-based methods, allow for the fabrication of plasmonic nanostructures but inherently suffer from edge blurring[12–14] and cannot produce plasmonic films perforated with nanoholes, which play an important role in nanoplasmonics.[15] Nanoimprint lithography[16,17] and soft lithography[18] have been used to efficiently nanopattern the surface of silk films,[6] but have not yet succeeded in the demonstration of metallic nanostructures with complex geometry on a large footprint area. The most promising procedure for integrating plasmonic structures onto biopolymers is the technique known as nanotransfer printing (nTP). The nTP techniques previously developed utilize contact printing, relying on tailored surface chemistries to transfer metal films from the raised regions of a stamp to a substrate when these two elements are brought into contact.[19,20] Since its discovery, nTP has been used to fabricate nanoscale electrical contacts,[21] surface-enhanced Raman spectroscopy (SERS) substrates,[22] 3D multilayer metamaterials,[23] and other devices where the fabrication of metallic nanostructures is necessary; however to date, it has yet to be successfully applied to bioactive silk films.

D. Lin, Prof. L. Dal Negro
Department of Electrical and Computer Engineering & Photonic Center
Boston University
Boston, MA 02215, USA
E-mail:dalnegro@bu.edu
Prof. D. L. Kaplan, Prof. F. G. Omenetto, Dr. H. Tao, Dr. J. P. Mondia
Department of Biomedical Engineering
Tufts University
4 Colby Street, Medford, MA 02155, USA
J. Trevino, Prof. L. Dal Negro
Division of Materials Science and Engineering
Boston University
Brookline, MA 02446, USA
Prof. F. G. Omenetto
Department of Physics
Tufts University
4 Colby Street, Medford, MA 02155, USA

DOI: 10.1002/adma.201201888

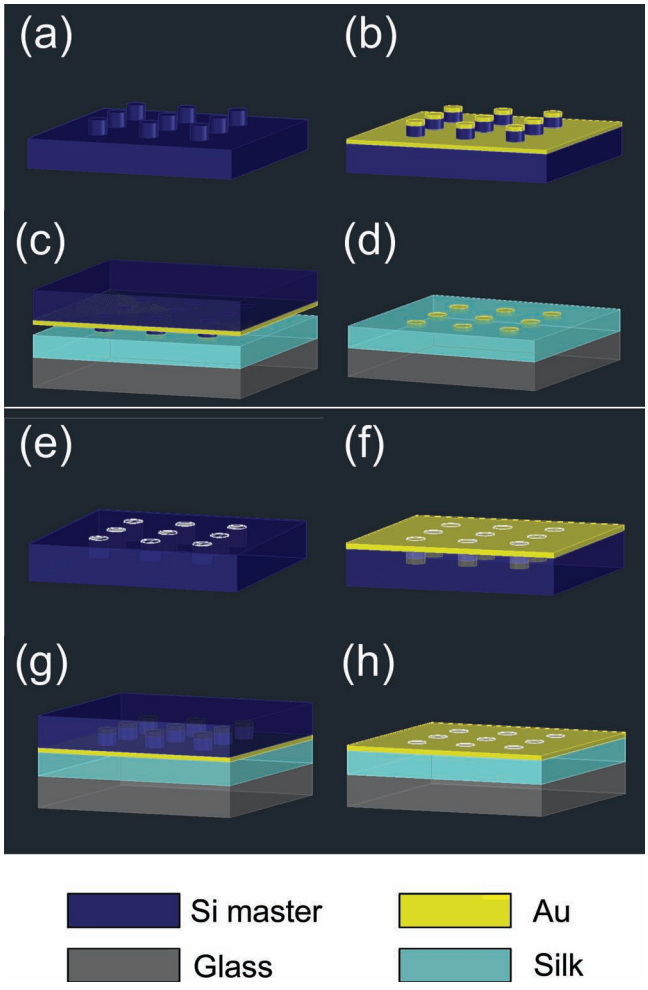

Figure 1. Process flow of transfer nanoimprint of plasmonic nanostructures using reusable masters. (a-d) Plasmonic nanodot structures and (e-h) plasmonic nanohole structures. (a,e) Pillar and hole structures defined in Si master by EBL and RIE processing. (b,f) E-beam evaporation of Au films to be transfered. (c,g) Transfer imprint utilizing commercial flip-chip bonder. (d,h) Removal of master, leaving Au nanodot and nanohole arrays on the silk film surface.

In this paper, we propose and demonstrate a scalable and cost-effective direct transfer nanofabrication technique that utilizes a hard mold master and an inexpensive, commercially available flip-chip bonder, for the fabrication of large-scale metallic nanoparticles (plasmonic nanodots) and perforated metallic films (plasmonic nanoholes) on silk fibroin films. Moreover, the proposed technique enables the fabrication of arbitrarily complex nanostructures with deep subwavelength spatial resolution down to 40 nm over large areas and with high throughput, while maintaining the optical functionality of silk films. To demonstrate the flexibility of the process, we show transfer imprint of both periodic and aperiodic arrays of plasmonic nanodots, nanoholes, and bow tie nanoantennas atop light emitting silk substrates doped with RhB. The preservation of the distinctive scattering resonances of metallic aperiodic arrays when patterned directly on silk substrates and the demonstration of visible fluorescence enhancement by the imprinted plasmonic structures prove the first successful integration of nanoplasmonic arrays with biopolymers of silk films.

The process flow for the transfer imprint of plasmonic nanodots and nanoholes, sketched in **Figure 1**, begins with the fabrication of the reusable master molds. In the case of the nanodot transfer process, the desired geometry is fabricated into a Si mold consisting of nanopillar arrays (Figure 1a), while the nanohole process requires a mold containing nanoholes (Figure 1e). The designed arrays are first defined by EBL in a PMMA film. Details on the EBL master fabrication are described in the Experimental Section. The nanodot master fabrication proceeds with the deposition of 35 nm-thick chrome (Cr) layer via electron beam (e-beam) evaporation, followed by a lift-off process in heated acetone. The resulting Cr nanocylinders serve as a etch mask for a 230 nm-deep anisotropic reactive ion etch (RIE), forming the desired nanopillar array. The residual Cr layer is then removed by wet chemical etch. **Figures 2**a and b show scanning electron microscopy (SEM) images of nanodot and nanohole masters for the replication of α_1 aperiodic Vogel spiral arrays.[24] Arrays with complex Vogel spiral geometry, featuring a high density of spatial frequencies, are selected to demonstrate the potential of the direct transfer technique.[24–26] Nanopillar diameters are measured to be 250 nm, the minimum particle spacing is 40 nm, and the linear array diameters range from 25 to 50 μm. The fabrication of the nanohole master shown in Figure 2b proceeds via EBL writing with a 260 nm-deep RIE step, using the PMMA as an etch mask. The remaining PMMA is removed by hot acetone bath, resulting in the Si nanohole master, shown in Figure 2b for the α_1 Vogel spiral configuration. Hole and geometrical array dimensions are the same as those for pillar arrays.

The Si masters were first treated with a silanizing agent to reduce the adhesion of the Au to the Si surface.[27] This surface treatment enables a higher yield in pattern transfer of the Au to the silk film in subsequent steps. The process flow continues with the deposition of a 35 nm-thick e-beam evaporated gold (Au) film, as shown in Figures 1b and 1f. The Au e-beam evaporation is highly anisotropic, resulting in negligible accumulation on the sidewalls of the etched structures, and restricting transfer of only raised features of the array in subsequent transfer steps. The Au coated masters are now ready for transfer imprinting on the silk films. In this study, we utilize a 600 nm-thick Rhodamine B (RhB) doped silk film, the preparation of which is described elsewhere.[9] A commercial flip-chip bonder (Smart Equipment Technology FC150) was employed to transfer imprint from the fabricated master molds. The flip-chip bonder is used to align and bond one or more chips onto a substrate using pressure and heat as shown in Figures 1c and 1g.

The transfer imprint process begins by heating the Au covered master to 90°C, when it is then pressed onto the surface of the doped silk film with a force of 30.6 MPa for 5 min. The transfer temperature was maintained near the glass transition temperature (T_g) of silk (~100 °C). Temperatures above 100 °C create a noncompatible environment for active biopolymers and are thus avoided. Transfer imprints performed at pressures below the optimized value resulted in low yield of transferred patterns. Those performed above the optimized value resulted

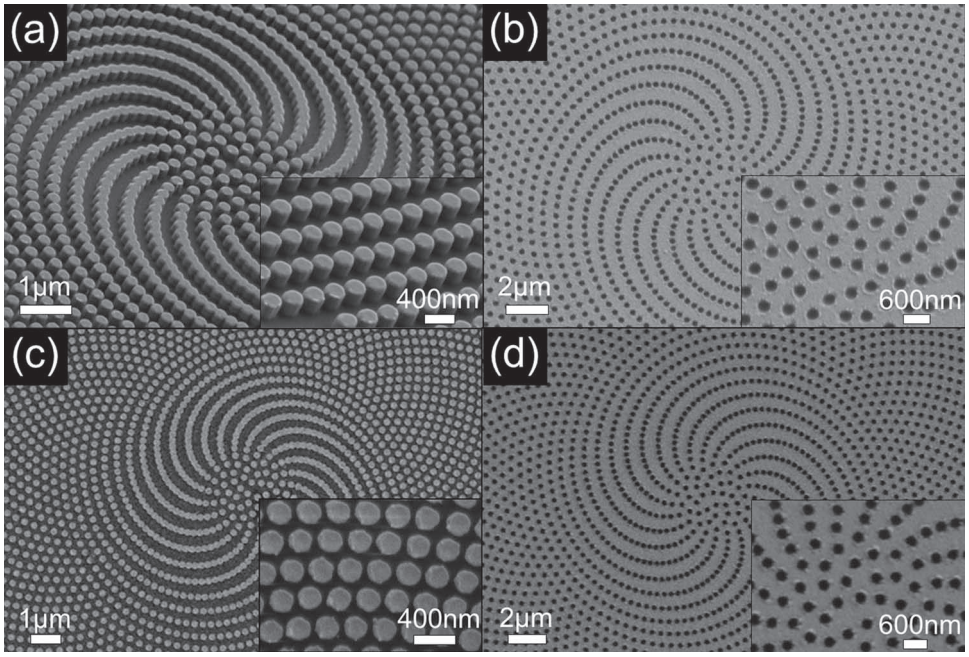

Figure 2. (a) SEM images of Si master Vogel spiral nanopillar array (α_1 spiral) used for transfer imprint of plasmonic nanodot structures (b) SEM images of Si master Vogel spiral nanohole array (α_1 spiral) used for transfer imprint of plasmonic nanohole structures. (c) Transferred plasmonic α_1 spiral nanodot array on silk film from Si master in a). (d) Transferred plasmonic α_1 spiral nanohole array on silk film from Si master in b).

either in Au incorporation into the silk films or, for sufficiently high pressures, in the delamination of the silk film. Leveling of the substrates is controlled through a system calibration to prevent the master from contacting the silk film at an angle, resulting in undesired pressure gradients. During the imprinting, the plasmonic nanostructures bind to the surface of silk film. The adhesion mechanism between the Au patterns and the silk films is currently under investigation,[27] although the presence of cysteine (Cys) residues in the silk macromolecule[28] could affect the surface energy of the film towards favoring thiol bonds of the Cys with Au.[29] Upon completion of the bonding cycle, the master is removed, leaving the Au embedded on the surface of the silk film as shown in 2c and 2d for nanodots and hole arrays, respectively. In this study, to demonstrate the successful integration of bioactive silk films and plasmonic nanostructures and the flexibility of the proposed technique, we have additionally imprinted nanodot and nanohole arrays in the form of bow tie nanoantennas, nanocylinders, as well as aperiodic Vogel spiral structures with varying morphology and interparticle separations. Bow tie nanoantenna arrays are of great interest in sensing and fluorescence enhancement applications due to their unique triangular geometry which leads to "lightening-rod" effects causing intense near-fields at the metal tips.[30,31] Here we demonstrate the ability to rapidly reproduce large arrays of bow tie antennas on active silk films with gap apex as small as 40 nm (**Figure 3**b). Periodic cylinder arrays are the most commonly utilized geometries in plasmonics, allowing for the engineering of plasmon enhanced fields in spectral regions where evanescent diffraction grating orders spectrally overlap the broader localized surface plasmon (LSP) resonances of the metallic nanoparticles. Figure 3 displays the SEM images of representative types of transfer imprinted nanodot (a) and nanohole (c-d) arrays.

It is important to note that the transfer imprint process can be repeated multiple times using the same master, reproducing structures with a high degree of fidelity. Array sizes are only limited by the user's ability to fabricate larger master substrates and, in principle, could scale up to the entire Si wafers if industrial EBL tools are to be utilized. After imprinting, residual Au left in the cavities of the master can be removed through a simple 10 minute wet Au etch step. The imprint process can then be restarted at the Au e-beam evaporation step as previously described. This is demonstrated in **Figure 4**, where we show the SEM images of the same Au dot pattern, consisting of an aperiodic golden angle Vogel spiral,[24,32] printed 3 times using the original master mold. The advantage of a reusable master allows high throughput and significant fabrication cost reduction. Moreover, the process final throughput can be significantly improved by automation of cleaning, metallization and imprint processes, as currently achieved with existing industrial equipment.

Vogel spiral arrays are attracting a growing interest due to their unique scattering and mode localization properties.[24–26,32,33] Recently, distinctive scattering resonances carrying orbital angular momentum have been discovered in nanoplasmonic Vogel spiral arrays, resulting in polarization-insensitive light diffraction and light emission enhancement across a broad spectral range.[24–26] More recently, localized optical modes with intriguing multifractal scaling properties have also been discussed.[33] In the Supporting Information, we show the optical resonances, imaged using white-light dark-field microscopy, of the transfer imprinted Vogel spirals. We

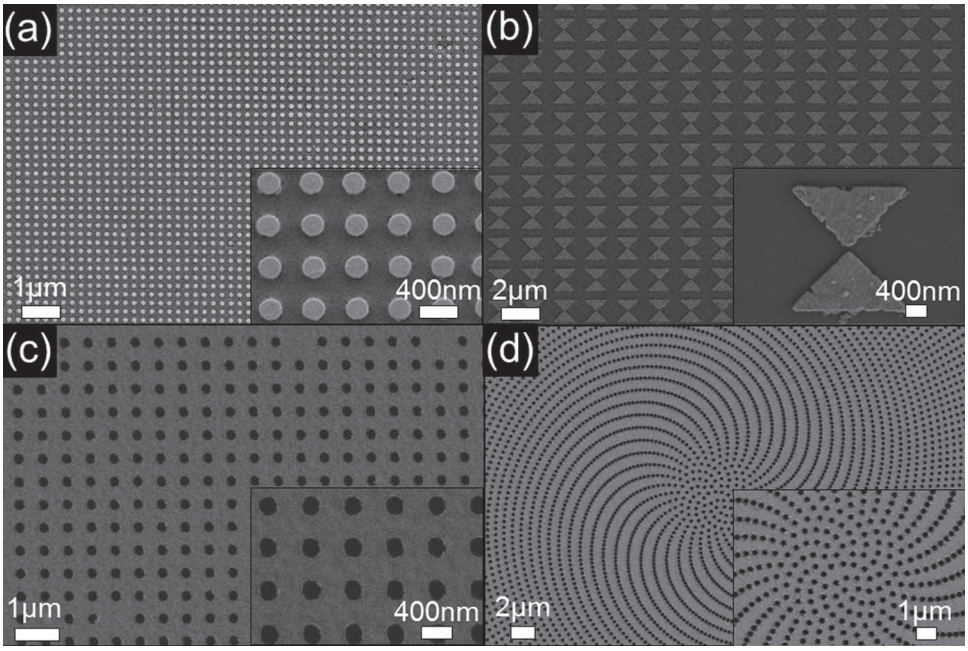

Figure 3. SEM images of transfer imprinted plasmonic nanodot arrays on doped silk fibrion films: (a) Periodic pattern of a = 400 nm and (b) bow tie structures with gap of 40 nm. SEM images of transfer imprinted plasmonic nanohole arrays on doped silk fibrion films: (c) Periodic pattern of a = 600 nm and (d) α_2 spiral array with a_{ave} = 308 nm.

notice that these scattering resonances closely correspond to the ones measured in samples fabricated by direct EBL writing on quartz substrates.[24]

Finally, the transfer imprint of plasmonic nanostructures is applied to fluorescence enhancement from RhB-doped silk films. The dye molecules were homogeneously doped into silk films by incorporating RhB dyes into the silk solution. The preparation of dye-doped silk films is described elsewhere.[9] It has been previously demonstrated that periodic dielectric nanostructures can be utilized to enhance the fluorescence of dye-doped silk films by a factor of 2 through the coupling to guided mode resonances created by the dielectric nanostructures.[9] By imprinting plasmonic nanostructures on dye-doped silk films, we demonstrate that larger values of fluorescence enhancement can be achieved by the excitation of LSPs in Au nanodot arrays.

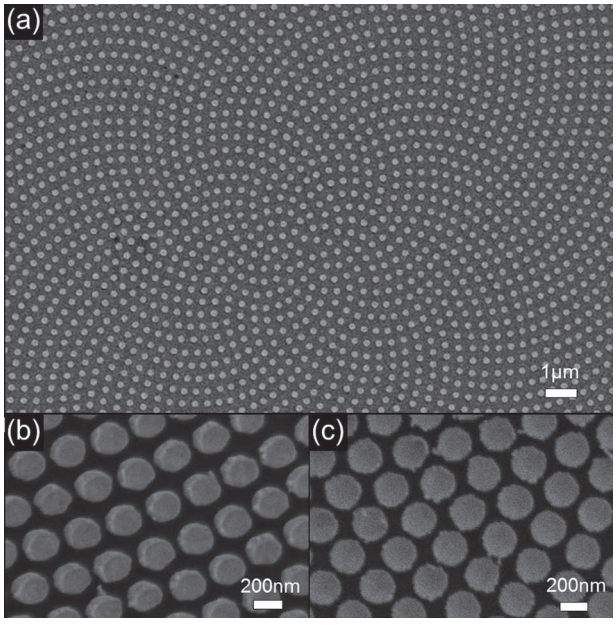

Figure 4. (a) SEM images of nanodot transfer imprinted GA spiral array with a_{ave} = 385 nm. (b) Close up SEM images of nanodot transferred array after (b) one use of the Si master and (c) three uses of the same Si master.

In **Figure 5**a, we show the fluorescence enhancement spectra measured on periodic, golden angle (GA), α_1, and α_2 spiral arrays with optimized structural parameters for visible light extraction. The emission spectra are collected as described elsewhere.[9] Fluorescence enhancement values are calculated by comparing the signal emitted by the patterned and unpatterned doped silk film. Figures 5(b-e) show the multispectral fluorescence images of imprinted plasmonic nanodots with different separations. The highest enhancement measured in a periodic array was found to be 4.4-fold for arrays with a grating constant of 400 nm, more than twice the value reported for dielectric imprinted arrays of the same dimensions.[9] The fluorescence enhancement measured in periodic arrays is a direct result of resonant coupling between the dopant emission in the silk film and the grating modes supported by the periodic array. Such an enhancement mechanism is highly sensitive to the matching of mode k-vectors to spatial frequencies corresponding to the Bragg peaks of the array structure. In contrast, GA Vogel spirals possess a Fourier space with diffuse circular rings,[24] that enables efficient extraction of randomly oriented dipole emission over a broader frequency spectrum.[25,26] As a result, when

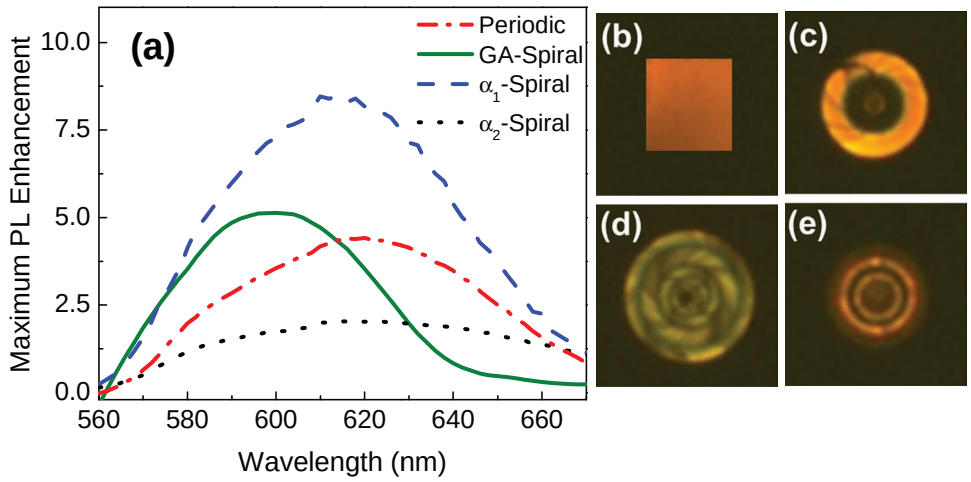

Figure 5. (a) Localized fluorescence enhancement spectra for transfer imprinted nanodots arrays pictured in Figure b)-e). Multi-spectral fluorescence images of transfer imprinted nanodot (b) periodic array with $a = 400$ nm, (c) α_1 spiral with $a_{ave} = 260$ nm, (d) GA spiral with $a_{ave} = 342$ nm, and (e) α_2 spiral with $a_{ave} = 200$ nm.

the spatial frequencies of GA and α_1 spirals are engineered to match the emission wavelength range of the RhB-doped film, significantly larger values of emission enhancement up to 8.5-fold have been experimentally measured.

In conclusion, we have successfully fabricated Au plasmonic nanostructures on doped silk films via a transfer imprint process, utilizing a commercially available flip-chip bonder. Compared to conventional inorganic photonic devices, silk films can be easily functionalized, providing added functions and selectivity. The developed transfer imprint method overcomes the challenges of integrating plasmonic metallic nanostructures with biopolymers, without the use of resist processing or harsh fabrication conditions. The developed process offers the advantage of low-cost, high-resolution, and large-area processing through the utilization of reusable masters. Moreover, the method is applicable to the fabrication of both plasmonic nanodot and nanohole structures that are currently not achievable using other biocompatible processes, such as shadow masking. In addition, complex aperiodic patterns with varying morphologies and interparticle separations can be reliably fabricated and their application to broadband fluorescence enhancement is demonstrated using silk-doped films.

These findings successfully demonstrate cost-effective and scalable integration of nanoplasmonics and optical silk technologies for the engineering of novel biocompatible optical materials and biophotonics devices.

Experimental Section

Electron Beam Lithography: The electron beam lithography (EBL) process begins with the spin-coating of a poly(methyl methacrylate) (PMMA, MicroChem A3 950) solution onto a silicon substrate for 10 s at 500 rpm and 45 s at 1500 rpm, followed by a hotplate bake for 1.5 min at 180 °C. The nanopatterns are then written using a Zeiss SUPRA 40VP SEM equipped with Raith beam blanker and NPGS for nanopatterning, with a dose of 400 μC cm^{-2} with proximity correction under a beam current of 31 pA at 30 keV. The exposed film is then developed in a 1:3 methylisobutyle ketone: isopropyl alcohol (MIBK:IPA) solution for 70 s. Afterwards, residual PMMA is removed by a 30 second reactive ion etch in oxygen plasma at 50 sccm and 50 mTorr with 200W RF power. The EBL process is then complete and the sample is ready for subsequent metallization steps.

Supporting Information

Supporting Information is available from the Wiley Online Library or from the author.

Acknowledgements

This work was supported by the AFOSR project "Deterministic Aperiodic Structures for On-chip Nanophotonic and Nanoplasmonic Device Applications" under Award FA9550-10-1-0019, and by the U.S. Army Research Laboratory and the U.S. Army Research Office under contract number W911NF-07-1-0618 and by the DARPA-DSO.

Received: May 9, 2012
Revised: July 11, 2012
Published online: September 3, 2012

[1] G. H. Altman, F. Diaz, C. Jakuba, T. Calabro, R. L. Horan, J. Chen, H. Lu, J. Richmond, D. L. Kaplan, *Biomaterials* **2003**, *24*, 401.
[2] F. G. Omenetto, D. L. Kaplan, *Nat. Photonics* **2008**, *2*, 641.
[3] D-H. Kim, J. Viventi, J. J. Amsden, J. Xiao, L. Vigeland, Y.-S. Kim, J. A. Blanco, B. Panilaitis, E. S. Frechette, D. Contreras, D. L. Kaplan, F. G. Omenetto, Y. Huang, K.-C. Hwang, M. R. Zakin, B. Litt, J. A. Rogers, *Nat. Mater.* **2010**, *9*, 511.
[4] D. H. Kim, Y. S. Kim, J. Amsden, B. Panilaitis, D. L. Kaplan, F. G. Omenetto, M. R. Zakin, J. A. Rogers, *Appl. Phys. Lett.* **2009**, *95*, 133701.
[5] F. G. Omenetto, D. L. Kaplan, *Science* **2010**, *329*, 528.
[6] B. D. Lawrence, M. Cronin-Golomb, I. Georgakoudi, D. L. Kaplan, F. G. Omenetto, *Biomacromolecules* **2008**, *9*, 1214.
[7] S. T. Parker, P. Domachuk, J. Amsden, J. Bressner, J. A. Lewis, D. L. Kaplan, F. G. Omenetto, *Adv. Mater.* **2009**, *21*, 2411.

[8] H. Perry, A. Gopinath, D. L. Kaplan, L. Dal Negro, F. G. Omenetto, *Adv. Mater.* **2008**, *20*, 3070.
[9] J. P. Mondia, J. J. Amsden, D. M. Lin, L. Dal Negro, D. L. Kaplan, F. G. Omenetto, *Adv. Mater.* **2010**, *22*, 4596.
[10] J. J. Amsden, P. Domachuk, A. Gopinath, R. D. White, L. Dal Negro, D. L. Kaplan, F. G. Omenetto, *Adv. Mater.* **2010**, *22*, 1746.
[11] S. A. Maier, in *Plasmonics: Fundamentals and Applications*, Springer, Berlin **2007**.
[12] S. Aksu, A. A. Yanik, R. Adato, A. Artar, M. Huang, H. Altug, *Nano Lett.* **2010**, *10*, 2511.
[13] O. Vazquez-Mena, T. Sannomiya, L. G. Villanueva, J. Voros, J. Brugger, *ACS Nano* **2011**, *5*, 844.
[14] H. Tao, J. J. Amsden, A. C. Strikwerda, K. Fan, D. L. Kaplan, X. Zhang, R. D. Averitt, F. G. Omenetto, *Adv. Mater.* **2010**, *22*, 3527.
[15] C. Genet, T. W. Ebbesen, *Nature* **2007**, *445*, 39.
[16] S. Y. Chou, P. R. Krauss, P. J. Renstrom, *Science* **1996**, *272*, 85.
[17] L. J. Guo, *Adv. Mater.* **2007**, *19*, 495.
[18] Y. Xia, G. M. Whitesides, *Ann. Rev. Mater. Sci.* **2008**, *28*, 153.
[19] Y. -L. Loo, R. L. Willett, K. W. Baldwin, J. A. Rogers *J. Am. Chem. Soc.* **2002**, *124*, 7654.
[20] Y. -L. Loo, R. L. Willett, K. W. Baldwin, J. A. Rogers, *Appl. Phys. Lett.* **2002**, *81*, 562.
[21] Y. -L. Loo, D. V. Lang, J. A. Rogers, J. W. P. Hsu, *Nano Lett.* **2003**, *3*, 913.
[22] N. A. Abu Hatab, J. M. Oran, M. J. Sepaniak, *ACS Nano* **2008**, *2*, 377.
[23] D. Chanda, K. Shigeta, S. Gupta, T. Cain, A. Carlson, A. Mihi, A. J. Baca, G. R. Bogart, P. Braun, J. A. Rogers, *Nat. Nanotechnol.* **2011**, *6*, 402.
[24] J. Trevino, H. Cao, L. Dal Negro, *Nano Lett.* **2010**, *11*, 2008.
[25] N. Lawrence, J. Trevino, L. Dal Negro, *J. Appl. Phys.* **2012**, *111*, 113101.
[26] E. F. Pecora, N. Lawrence, P. Gregg, J. Trevino, P. Artoni, A. Irrera, F. Priolo, L. Dal Negro, *Nanoscale* **2012**, *4*, 2863.
[27] K. Tsioris, H. Tao, M. Liu, J. A. Hopwood, D. L. Kaplan, R. D. Averitt, F. G. Omenetto, *Adv. Mater.* **2011**, *23*, 2015.
[28] C. Zhou, F. Confalonieri, M. Jacquet, R. Perasso, Z. Li, J. Janin, *Proteins: Struct., Funct., Bioinf.* **2001**, *44*, 119.
[29] C. Bain, E. Troughton, Y. Tao, J. Evall, G. M. Whitesides, R. Nuzzo, *J. Am. Chem. Soc.* **1989**, *111*, 321.
[30] R. D. Grober, R. J. Schoelkopf, D. E. Prober, *Appl. Phys. Lett.* **1997**, *70*, 1354.
[31] A. Sundaramurthy, K. B. Crozier, G. S. Kino, D. P. Fromm, P. J. Schuck, W. E. Moerner, *Phys. Rev. B* **2005**, *72*, 165409.
[32] M. E. Pollard, G. Parker, *J. Opt. Lett.* **2009**, *34*, 2805.
[33] J. Trevino, S. F. Liew, H. Noh, H. Cao, L. Dal Negro, *Opt. Express* **2012**, *20*, 3015.